Cell Reports, Volume *33*

Supplemental Information

TFEB Transcriptional Responses Reveal Negative Feedback by BHLHE40 and BHLHE41

Kimberly L. Carey, Geraldine L.C. Paulus, Lingfei Wang, Dale R. Balce, Jessica W. Luo, Phil Bergman, Ianina C. Ferder, Lingjia Kong, Nicole Renaud, Shantanu Singh, Maria Kost-Alimova, Beat Nyfeler, Kara G. Lassen, Herbert W. Virgin, and Ramnik J. Xavier

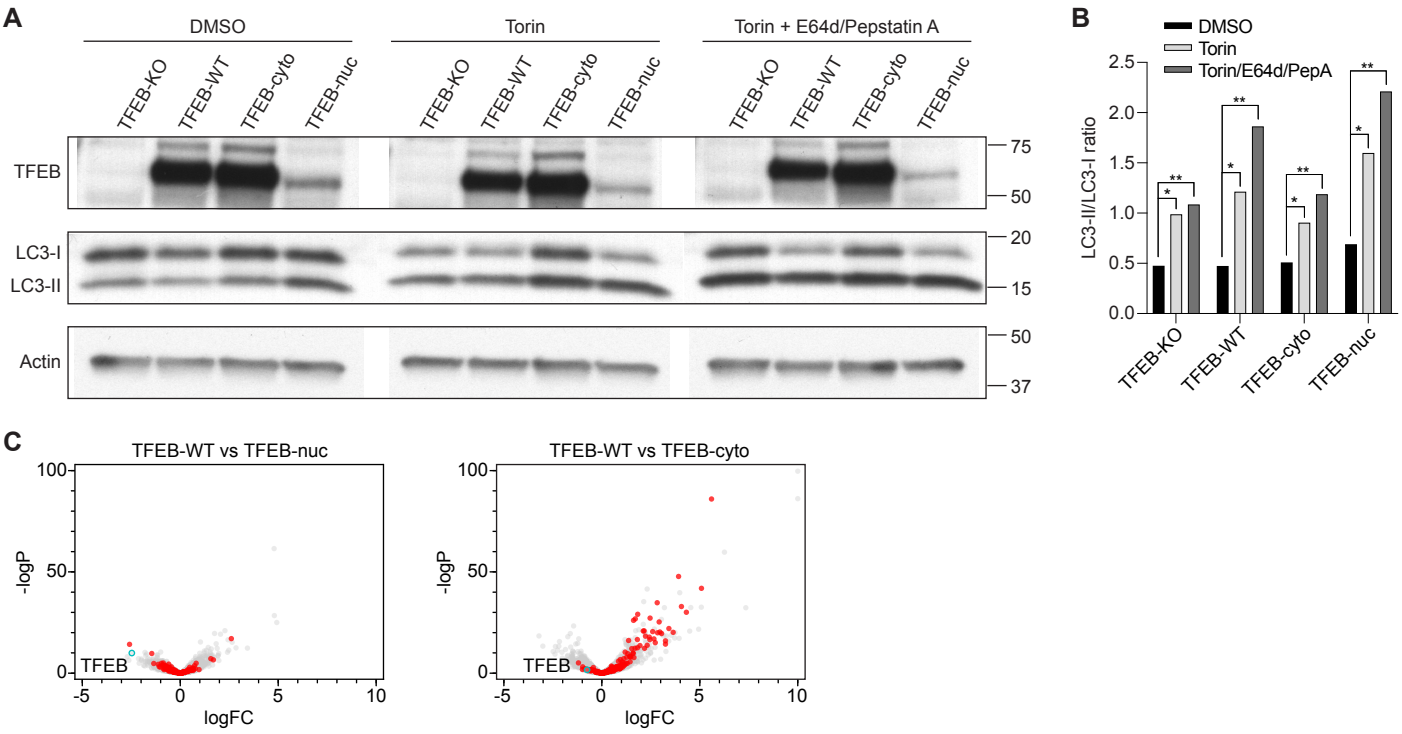

Figure S1. TFEB nuclear translocation is necessary for robust autophagy induction and transcriptional response. Related to Figure 1. Representative immunoblot **(A)** and quantification **(B)** of LC3 conversion in TFEB-KO and reconstituted HeLa cell lines treated with DMSO (0.1%), Torin (1μM), or a combination of Torin and E64d/Pepstatin A for 4hrs. Quantification of LC3-II/LC3-I ratio was normalized to actin loading control. Data are representative of three independent experiments and were analyzed using ordinary two-way ANOVA and Tukey's multiple comparisons test with individual variances for each comparison. Data are represented as mean +/- SEM (standard error of the mean). *p<0.05, **p<0.01. **C)** Cells were processed for RNA sequencing. Transcriptional responses to TFEB expression and localization are shown in volcano plots, where TFEB transcript is shown in cyan and a subset of known TFEB target genes (Table S1) (Sardiello et al., 2009) are shown in red.

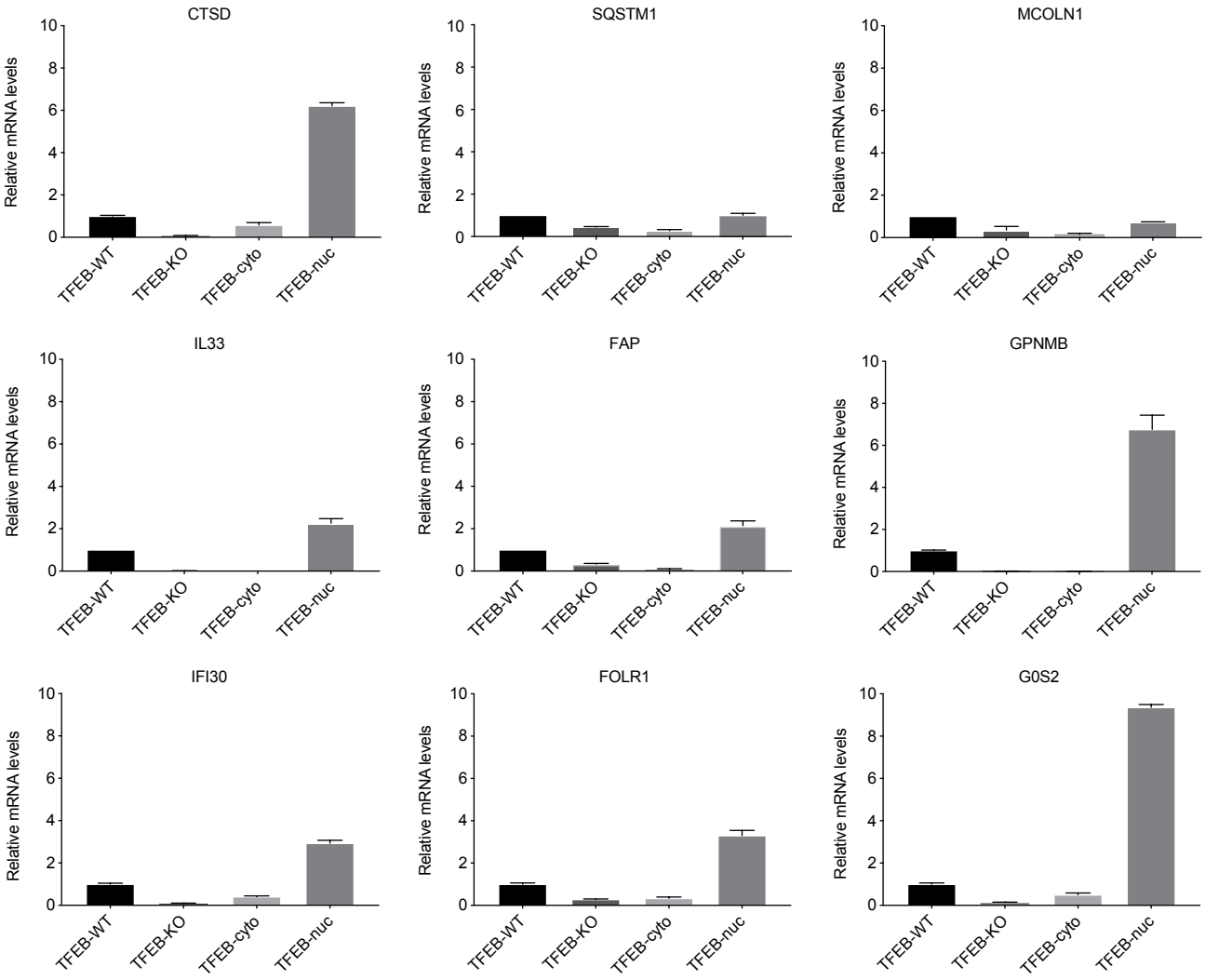

Figure S2. Quantitative PCR analysis confirms TFEB target genes are upregulated in response to TFEB nuclear localization. Related to Figure 2 and Table S2. Gene expression of select TFEB target genes in TFEB-KO, TFEB-WT, TFEB-cyto, and TFEB-nuc cells as quantified by qRT-PCR. Data shown are the average of duplicate wells and representative of three independent experiments. Data are represented as mean +/- SEM (standard error of the mean).

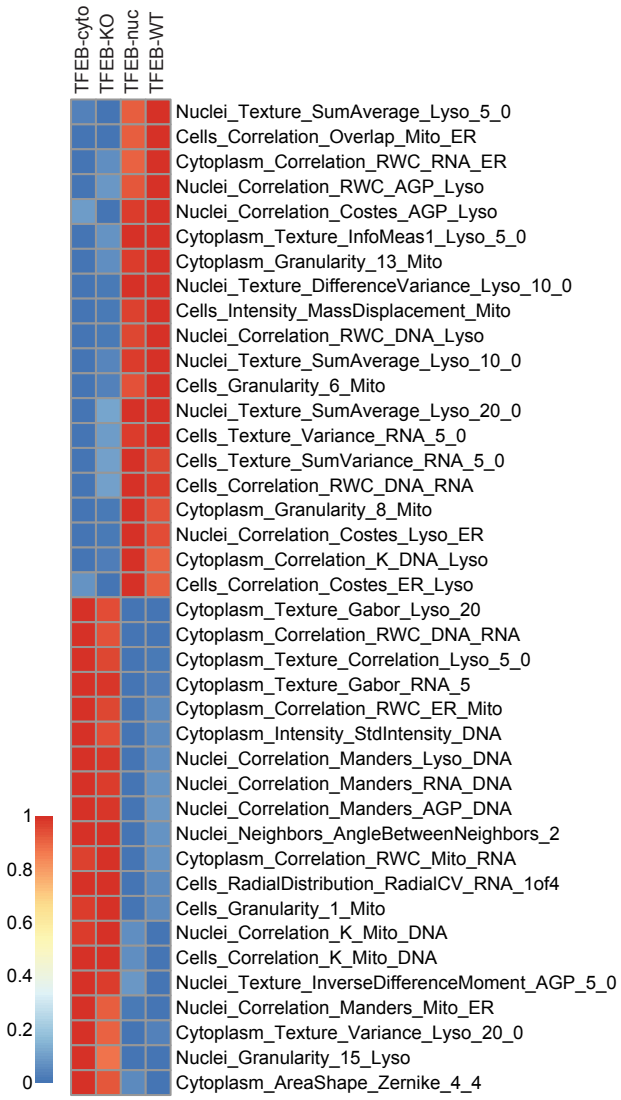

Figure S3. Cell Painting analysis identifies subcellular phenotypic responses to TFEB expression and localization. Related to Figure 3. Heat map representing Morpheus analysis of the most significant cellular features by t-test illustrates phenotypic differentiation of TFEB-WT/TFEB-nuc from TFEB-KO/TFEB-cyto cells. Columns indicate cell type and rows indicate Cell Painting features [Compartment]_[FeatureGroup]_[Feature]_[Channel]_[Parameters] (Bray et al., 2016).

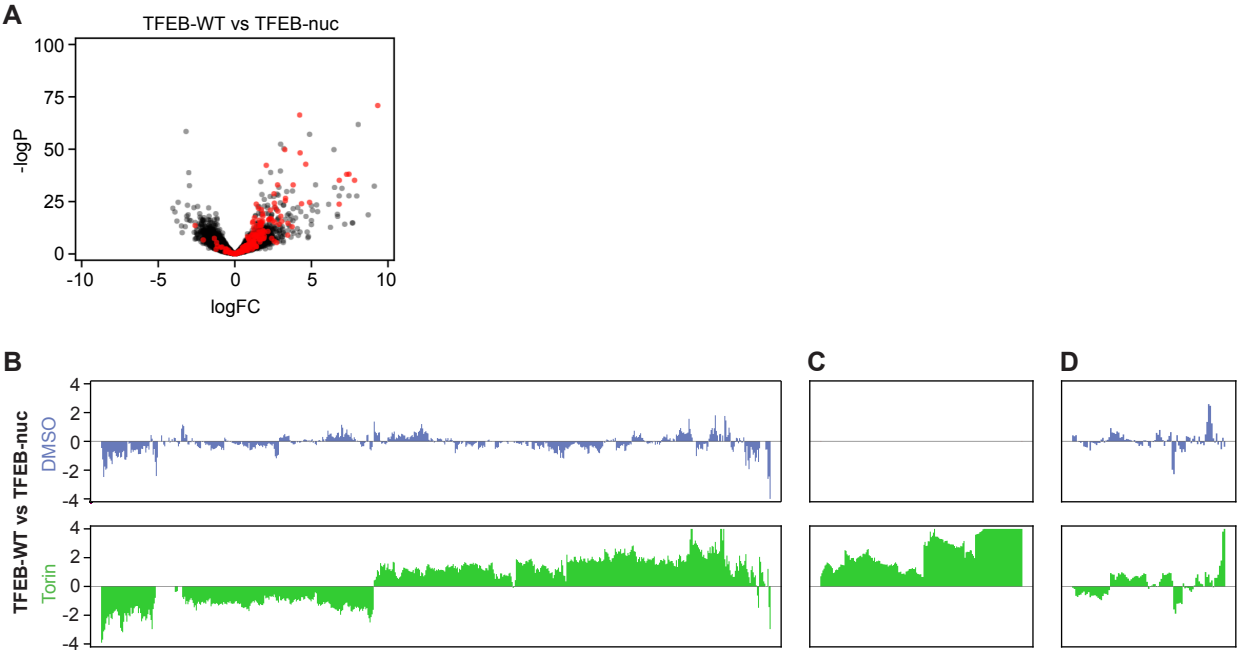

Figure S4. Expression of TFEB-WT, but not TFEB-nuc, upregulated transcription in response to Torin treatment. Related to Figure 4 and Table S4. A) Volcano plot of genes differentially expressed in TFEB-WT cells as compared to TFEB-nuc following Torin treatment. Shown in red are a subset of known TFEB target genes (Table S1) (Sardiello et al., 2009). **B-D)** Panels show differential gene expression at steady-state (DMSO, blue) and with Torin treatment (green). Each bar corresponds to a gene, and the y-axis represents log fold change of differential gene expression (truncated logFC+/-ln4). Genes represented in the bar plots are all genes with significant differential expression (logFC>ln4 or logFC<-ln4 and q-value<0.01) in TFEB-WT relative to TFEB-nuc following Torin treatment. Panel **B** represent genes significantly upregulated with Torin treatment, panel **C** represents genes significantly upregulated with Torin treatment and not transcribed at detectable levels without Torin stimulation, and panel **D** represents TFEB-dependent genes for which transcription did not significantly change in response to Torin stimulation.

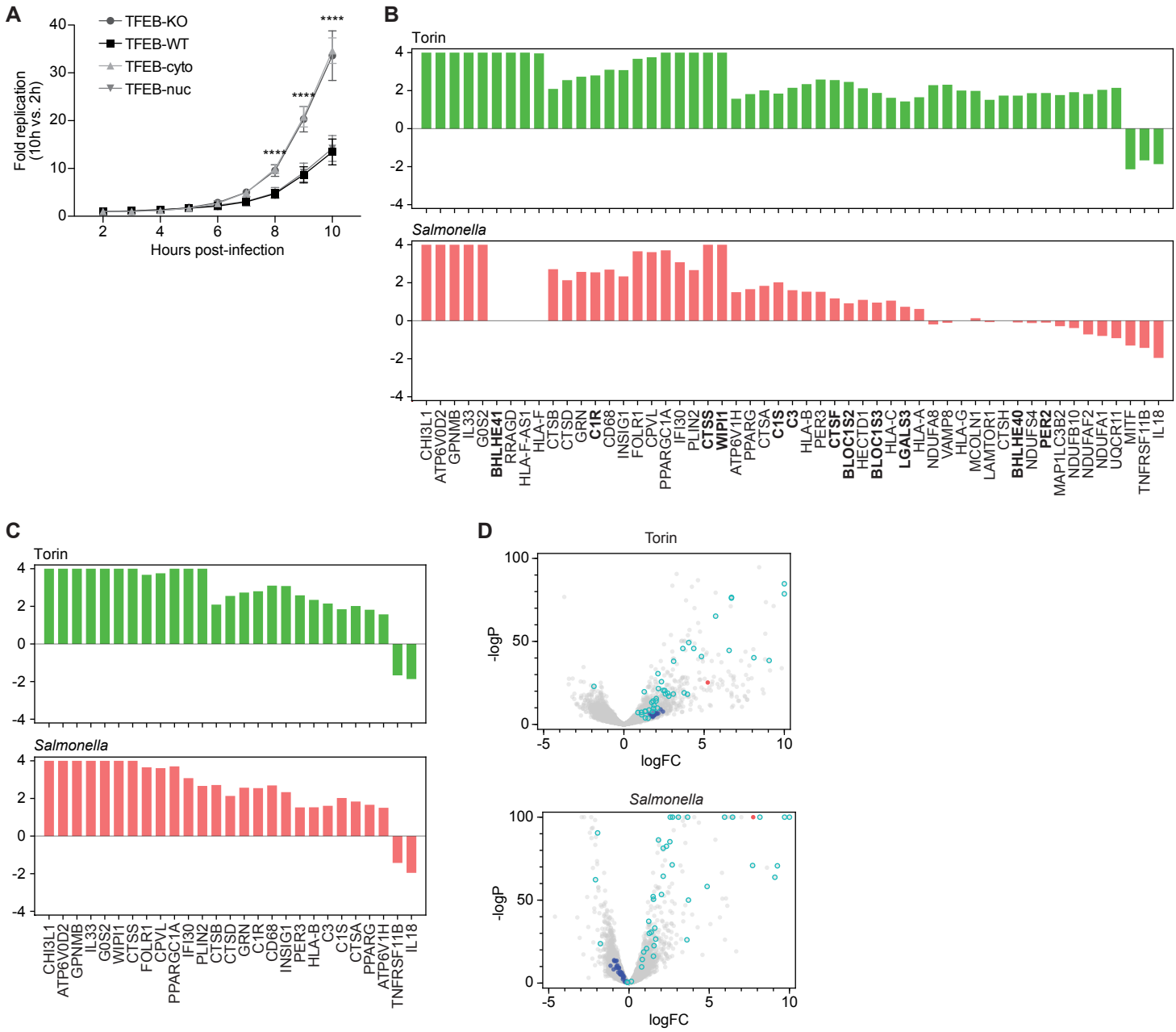

Figure S5. TFEB nuclear translocation is required for transcriptional response and host defense response to intracellular bacteria. Related to Figure 5. A) Intracellular bacterial replication in TFEB-KO, TFEB-WT, TFEB-cyto, and TFEB-nuc cells infected with bioluminescent *S. enterica*. Data shown are the average of eight independent wells and representative of three independent experiments. Data were analyzed using repeated measures two-way ANOVA with Geisser-Greenhouse correction and individual variances computed by Sidak's multiple comparisons test. Data are represented as mean +/- SEM (standard error of the mean). ****p<0.0001. **B)** TFEB-KO and TFEB-WT cells were treated with Torin or infected with *S. enterica* then processed for RNA sequencing analysis. Response of select genes differentially expressed between TFEB-WT and TFEB-KO cells following Torin treatment (logFC>ln4 or logFC<-ln4 and q-value<0.01) are shown. A subset of genes differentially expressed following Torin treatment (green) are also differentially expressed in cells infected with *Salmonella* (pink). **C)** TFEB-KO and TFEB-WT cells were treated with Torin or infected with *S. enterica* then processed for RNA sequencing analysis. Select genes differentially expressed between TFEB-WT and TFEB-KO cells in response to both Torin treatment (green) and *Salmonella* infection (pink) (logFC>ln4 or logFC<-ln4 and q-value<0.01) are shown. **D)** Volcano plots illustrate differential gene expression from TFEB-KO and TFEB-WT cell lines treated with Torin (top) or infected with *S. enterica* (bottom). TFEB (red) and select genes functioning in autophagy, lysosome and immune responses (cyan) and mitochondrial respiration (blue) are highlighted.

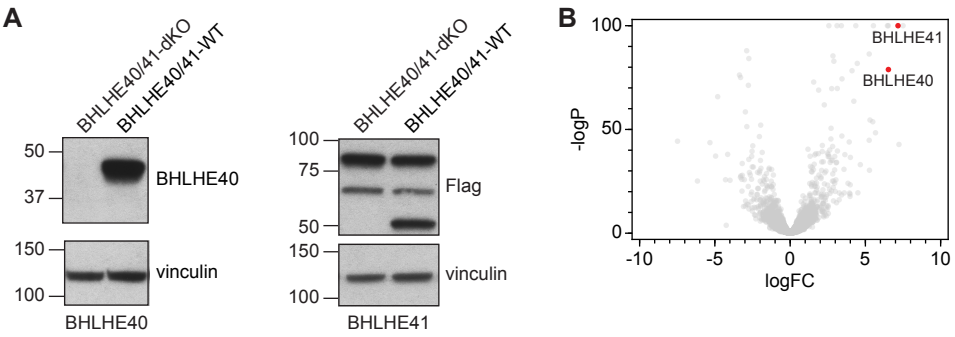

Figure S6. Re-expression of BHLHE40 and BHLHE41 in BHLHE40/41-dKO cells is detected by immunoblot and RNA sequencing. Related to Figure 7. A) Immunoblots demonstrate BHLHE40 and BHLHE41 proteins are detected with anti-BHLHE40 and anti-Flag antibodies, respectively, in BHLHE40/41-WT but not BHLHE40/41-dKO cells. Vinculin serves as a loading control. Data are representative of at least two independent experiments. **B)** BHLHE40/41-dKO and BHLHE40/41-WT cell lines were processed for RNA sequencing analysis. As compared to dKO cells, BHLHE40 and BHLHE41 transcript levels (red) are significantly increased upon reconstitution.